

# EFFECT OF MOBILITY RATIO ON PATTERN BEHAVIOR OF A HOMOGENEOUS POROUS MEDIUM

Y. Wang, A. R. Kavscek, and W. E. Brigham  
Department of Petroleum Engineering  
Stanford University  
Stanford, CA 94305-2220

## ABSTRACT

It is well known, for unit mobility ratio, that the areal sweep efficiency of a staggered-line-drive pattern is always better than a five-spot pattern. However, this observation does not hold for very favorable mobility ratios. We present simulation results and, with the help of streamline and saturation distributions, explain the differences between unit and favorable mobility ratios. Simulations compare well with experiments conducted elsewhere. Accurate definition of breakthrough time is also discussed for multiphase, streamline, simulation results. The exact definition of breakthrough is difficult due to physical dispersion in experiments and numerical dispersion in simulations.

## INTRODUCTION

Pattern geometry plays a major role in determining oil recovery during secondary and enhanced oil recovery operations. Although simulation is an important tool for design and evaluation, the first step often involves rough calculations based upon areal sweep efficiencies of displacements in homogeneous, two-dimensional, scaled, physical models<sup>1-3</sup>. These results are available as a function of the displacement pattern and the mobility ratio,  $M$ . The mobility ratio is simply the mobility of the displacing phase over that of the displaced, or resident, phase. Because it is possible to compute sweep efficiency analytically when the displacing and displaced phase have the same mobility<sup>4, 5</sup>, scaled physical model results have been verified for unit mobility ratios.

Convincing verification of the non-unit mobility ratio cases does not appear in the literature. Typical finite difference solutions of the reservoir flow equations suffer from numerical dispersion, the effects of which are hard to evaluate. Furthermore, the scaled physical model results at low mobility ratios ( $M \ll 1$ ) are provocative. For instance, Fig. 1a shows that recovery from a five-spot pattern at breakthrough for  $1/M$  greater than about 7.5 is virtually 100%, whereas recovery at breakthrough in Fig. 1b for a staggered-line-drive pattern at an  $1/M$  of 7.5 is a little more than 88%. This contradicts the common notion that areal sweep efficiency from a staggered-line-drive pattern is always better than that from a five-spot pattern.

We use a 3D streamline simulator<sup>6</sup> to analyze displacements in five-spot and staggered-line-drive patterns for stable displacements, that is  $M$  less than 1. In the following sections, we present streamline distributions, saturation distributions, and fractional flow at the producer versus dimensionless time,  $t_D$ . The dimensionless time is equal to the number of pore volumes of liquid

injected. With the streamline and saturation distributions at different times, we explain why and at what mobility ratio the five-spot pattern can recover more oil than a staggered-line-drive pattern.

The streamline calculation method is advantageous in that the results suffer from much less numerical dispersion than typical finite-difference approximations, but some dispersion in simulation results is evident. Therefore, we discuss how to treat the numerical dispersion to obtain accurate estimates of breakthrough times. We discuss the proper way to calculate fractional flow based on the flow rates at the producer. In comparing the simulation results with the experimental results of Dyes *et al*<sup>1</sup>, physical dispersion in the experiments is found even though a piston-like displacement was assumed.

### SWEEP EFFICIENCY

Before proceeding, it is useful to recall the representation of experimental data in Fig. 1 and the meaning of sweep efficiency. Dyes *et al.*<sup>1</sup> used various oils as both the injected and displaced phases. These hydrocarbons were miscible and they assumed piston-like displacement. An X-ray shadowgraph technique was used to observe the position of the displacing front. Areal sweep efficiencies are plotted versus displaceable pore volumes injected for different mobility ratios. In the figure, the x axis is the reciprocal of mobility ratio. Each curve in the graphs corresponds to a specific  $t_D / \Delta S$ , or displaceable pore volume injected. The bottom curves show sweep efficiencies at breakthrough. It is assumed that the displacement has a piston-like front and there is no physical dispersion. Likewise, the porous medium is assumed to be perfectly homogeneous.

For piston-like displacement, the areal sweep efficiency is

$$E_A = A_S / A_T \quad (1)$$

where  $A_S$  is the swept area and  $A_T$  is the total area. Before and at breakthrough, the amount of displacing fluid injected is equal to the displaced fluid produced, disregarding compressibility. Assuming piston-like displacement, injected volume is related to area swept

$$V_I = A_S h \phi \Delta S \quad (2)$$

where  $V_I$  is the volume of displacing fluid injected,  $h$  is the thickness of the formation, and  $\phi$  is porosity. Hence,

$$E_A = A_S / A_T = V_I / (A_T h \phi \Delta S) = t_D / \Delta S \quad (3)$$

where  $t_D = V_I / (A_T h \phi)$  is the pore volume of fluid injected, also commonly called dimensionless time. For  $\Delta S = 1$ ,  $E_A = t_D$  before and at breakthrough.

After breakthrough,

$$E_A = (V_I - V_P) / (A_T h \phi \Delta S) \quad (4)$$

where  $V_P$  is volume of displacing fluid produced.

## SIMULATION RESULTS

We use a three-dimensional streamline simulator, called 3DSL, written by Batycky *et al*<sup>6,7</sup> to simulate the displacement for the five-spot and staggered-line-drive patterns. It uses the pressure field to decompose the flow problem into a series of streamtubes that span from injector to producer and carry identical volumetric flowrates. In the simulations, we set the conditions identical to those in the experiments and choose relative permeability curves that ensure a piston-like displacement. The conditions are

1. Homogeneous permeability field, *i.e.*,  $k$  is constant.
2. Straight line relative permeability curves with end point relative permeability of 1, *i.e.*,  
$$k_{rw} = S_w, \quad k_{ro} = S_o \quad (5).$$
Therefore,  $k_{rw} + k_{ro} = 1$  for any  $S_w$ .
4. Mobility is altered by changing viscosity, and the mobility ratio is the reciprocal of viscosity ratio.
5. We set  $\Delta S = 1$  which means that ahead of the displacing front, the displacing phase saturation is zero, and behind the front, it is unity.

3DSL is very fast compared to conventional finite difference simulators and exhibits much less numerical dispersion<sup>6,7</sup>. For our problem, it offers us the streamline distribution which facilitates explanation of displacement behavior.

We use many pressure solves (time steps) and very fine uniform grids (100 by 100 cells for the five spot and 140 by 70 cells for the staggered line drive) to ensure converged simulation results. A grid refinement study showed these grids to be optimal in that further refinement of the grid did not yield noticeable changes in breakthrough time, the oil production curve, or displacement patterns<sup>8</sup>. For unit mobility ratio ( $M = 1$ ), we actually only need one pressure solve. But for mobility ratios far from 1, we need many pressure solves. For  $1/M = 20$ , we used up to 1000 pressure solves to ensure that the results were converged. In the streamline approach, a pressure solve is accompanied by a re-determination of streamline paths and, hence, the flow field on the underlying fixed grid.

Figure 2 displays areal sweep efficiencies as a function of pore volume injected for differing mobility ratios, and compares simulation and experimental results<sup>1</sup>. The solid lines are simulation results, solid circles experimental results, and dotted lines connect circles for ease of viewing. In this figure, we concentrate on only the favorable mobility ratios,  $M < 1$ . We noticed more numerical dispersion for unfavorable mobility ratio cases, not reported here.

Figure 3 shows the displacing fluid fractional flow at the producer as a function of dimensionless time for several mobility ratios. To compute fractional flow from the numerical data we use a central finite-difference formula rather than backward differences. The shapes of the fractional flow curves at breakthrough ( $t_D$  from roughly 0.7 to 1) indicate some numerical dispersion. We expect the fractional flow to increase sharply rather than gradually at water breakthrough. As expected, the numerical dispersion decreases as  $M$  becomes more favorable<sup>9</sup>. The most numerical dispersion occurs for unit mobility ratio, as shown in Fig. 3. We modify the breakthrough time by trimming the numerical dispersion as will be described next.

## BREAKTHROUGH DETERMINATION

Due to numerical dispersion, injected fluid breaks through earlier at the producer than it should. However, the numerical dispersion does not have much effect on the late-time displacing fluid production. The fractional flow versus  $t_D$  plots shown in Fig. 3 illustrate the early breakthrough caused by numerical dispersion.

To correct for numerical dispersion in breakthrough times and approximate the breakthrough time more accurately, we use fractional flow data after breakthrough which is relatively free from the effects of dispersion and extrapolate back to the breakthrough time. A least-squares method is used with second order polynomials:

$$t_D = a + bf_w + cf_w^2 \quad (6)$$

The data points employed lie between  $0.1 < f_w < 0.5$ . The dashed lines in Fig. 3 illustrate this procedure. All the breakthrough times reported here are modified using this method.

We caution that using the approach embodied in Eq. (6) to estimate the shape of the water-cut curve for times exceeding breakthrough incurs a mass balance error. The amount of production prior to breakthrough that is trimmed from the original data is not added back to the production curve at later times. For this reason, we use Eq. (6) only to estimate breakthrough time and not to analyze post breakthrough behavior.

Numerical dispersion is also related to the number of time steps (*i.e.*, pressure solves). In the streamline approach applied here, dispersion can be introduced through the process of mapping the streamline saturation distribution onto the underlying Cartesian grid used to compute the pressure field<sup>6</sup>. Hence, for a unit mobility ratio where the pressure field does not change, the most accurate results are obtained when a single time step is used. By performing various single time step simulations, we determine a breakthrough time of 0.7178 for the five spot ( $d/a = 1/2$ ) with  $M$  equal to 1. This is in good agreement with the analytical solution<sup>4</sup> of 0.7177. Likewise, analytically<sup>4</sup> and numerically determined breakthrough times for a staggered-line-drive ( $d/a = 1$ ) pattern are both equal to 0.785. With multiple time steps (50) breakthrough times were sooner, but using the method discussed above, we obtain the same values for the breakthrough times, at  $M = 1$ .

## DISCUSSION

Comparing simulation results and experimental results in Fig. 2, we notice that breakthrough occurs earlier in the experiments than predicted by the simulations. Note that the experimental breakthrough time for the five spot at unit mobility ratio is 0.70 while the simulated value agrees to within 4 significant figures with the analytical result. This discrepancy is consistent with physical dispersion in the experiments. For the staggered-line-drive pattern in Fig 2b, experimental data indicates that  $E_A$  at breakthrough is roughly 0.75 for  $M$  equal to 1. In the experiments, there is physical dispersion even though a piston-like front is assumed. In the simulation results presented in Fig. 2a, the sweep efficiency at breakthrough is 99.7% when  $1/M = 20$ . An almost negligible area immediately around the producer is not completely swept at breakthrough due to either a very small amount of dispersion in the simulations or perhaps cusping of the displacement front toward the production well (refer to Fig. 3, five spot,  $1/M = 20$ ).

After breakthrough, the differences in areal sweep efficiencies between the experiments and simulations become much smaller (Fig. 2). After breakthrough, the numerical dispersion consists of only a portion of the displacing fluid produced. As time increases, this portion decreases and the dispersion has less effect on areal sweep efficiency. However, the differences between the experimental results and the simulation results are consistent, i.e. the areal sweep efficiencies of the simulations are generally higher than those of the experiments. As shown in Fig. 2(a), the simulated breakthrough curve levels off at large  $1/M$  with near zero slope, and does not exceed 1. However, the experimental curve shows  $E_A$  equal to 1 at  $1/M$  equal to about 7.5. We note that in the plot drawn by Dyes *et al*, the point where the breakthrough curve hits the  $E_A$  equal to 1 line is only an extrapolation from other data points (refer to Fig. 8 of ref. <sup>1</sup> or equivalently Fig. 6-2 of ref <sup>3</sup>).

### Areal Sweep Efficiency

Figure 4 plots computed breakthrough,  $t_D$ , versus the conventional shape factor  $d/a$  for various mobility ratios. The analytical solution for the unit mobility ratio<sup>4</sup> is also plotted on the same figure for comparison. We find a good match of the sweep efficiency at breakthrough between the analytical solution and simulation results. The greatest differences are about 1% at  $d/a$  values of 0.75 and 3.0.

For unit mobility ratio, Fig. 4 teaches that a staggered-line-drive pattern ( $d/a = 1$ ) always has better areal sweep efficiency than a five-spot pattern ( $d/a = 1/2$ ). As the staggered-line-drive pattern becomes longer relative to its width ( $d/a$  increases), the displacement pattern approaches linear flow. High sweep efficiency results.

As the mobility ratio becomes more favorable, the advantage of staggered line drive on sweep efficiency diminishes. When the mobility ratio decreases to 0.2, the five-spot pattern becomes better than the staggered-line-drive pattern with  $d/a = 1$ . However, if  $d/a$  is increased, the staggered line drive recovery can be better than the five-spot pattern for this mobility ratio.

When the mobility ratio decreases to 0.05 or lower (very favorable), the areal sweep efficiency for the five-spot pattern is very close to 1 at breakthrough. That is, sweep out is complete at breakthrough. At this mobility ratio, the five-spot pattern is as good as a very long staggered line drive ( $d/a \approx 15$ , almost linear flow), and much better than the common staggered line drive ( $d/a = 1$ ). The transition point for five spot sweep efficiency exceeding that from a staggered line drive is around a mobility ratio of 0.3. When the mobility ratio is higher than 0.3, a staggered line drive is always better than a five spot. If mobility ratio is lower than 0.3, then the five spot can be higher in sweep efficiency than a staggered line drive.

These results are rooted in the geometry of each pattern. The symmetry of the five-spot pattern about the diagonal connecting injector and producer coupled with the favorable mobility ratio leads to almost perfect sweep of the pattern area at breakthrough. In the common staggered line drive, a portion of the pattern is always left unswept at breakthrough regardless of the mobility ratio. Increasing  $d/a$  of the staggered line drive reduces the fraction of the pattern volume that is not swept at breakthrough. Presentation and support of these observations form the core of discussion for the remainder of this paper.

The excellent displacement from a five-spot pattern for very favorable mobility ratios is explained with the help of streamline distributions. Streamlines are presented in equal increments of the stream function. Every pair of streamlines forms a stream tube, and the volumetric flow rate is the same in all of the stream tubes. Streamlines must extend from injector to producer. All of the stream tubes connect with the same injector and producer, and the pressure drop for all the

streamtubes is the same. With the same pressure drop and the same volumetric flow rate, the flow resistance is the same for all the streamtubes.

For our straight-line relative permeability assumption, we have

$$R_i = -\Delta p / q = \int_0^{L_i} \frac{\mu}{kA} dl \quad (7)$$

where  $R_i$  and  $L_i$  are the resistance and length of streamtube  $i$ , respectively, that vary with time. The quantity  $k$  is the homogeneous permeability and  $A$  is the cross sectional area of the streamtube. The cross-sectional area is

$$A = hw$$

where  $h$  is the constant thickness of the layer and  $w$  is the variable width of the streamtube.

Resistance in streamtube  $i$  is the same as that in streamtube  $j$  and thus

$$\int_0^{L_i} \frac{\mu}{kA} dl = C(t) \quad (8)$$

for all the streamtubes at a given time, where  $C(t)$  is constant. Moving the constant parameters  $k$  and  $h$  to the right hand side, we have

$$\int_0^{L_i} \frac{\mu}{w} dl = C(t) \quad (9)$$

For a piston-like displacing front,

$$\mu_1 \int_0^{l_{fi}} \frac{1}{w} dl + \mu_2 \int_{l_{fi}}^{L_i} \frac{1}{w} dl = C(t) \quad (10)$$

where  $\mu_1$  and  $\mu_2$  are the constant viscosities of the displacing and displaced fluids, respectively, and  $l_{fi}$  is the time-dependent distance from the injector to the displacing front.

### Unit Mobility Ratio

For a unit mobility ratio, the pressure field remains unchanged throughout the displacement, and so do the streamlines. The streamline distributions at  $M = 1$  for the five-spot and staggered-line-drive ( $d/a = 1$ ) patterns are shown in Fig. 5.

For unit mobility ratio, Eq. (10) is

$$\mu \int_0^{L_i} \frac{1}{w} dl = C \quad (11)$$

and  $C$  is independent of time. From Eq. 11, we know that if the  $i$ th streamtube is longer than the  $j$ th streamtube, then the average width of the  $i$ th streamtube  $w_i$  is greater to maintain the same

resistance and flow rate. Therefore, the volume of the  $i$ th streamtube is larger than the  $j$ th streamtube. The greater the difference in streamtube length, the bigger the difference in streamtube width, and, when breakthrough happens in the  $j$ th streamtube, the front has not progressed as far in the  $i$ th streamtube.

For a five-spot pattern, the longest streamline is that along the boundary, which is  $2a$ . The shortest streamline is the one along the diagonal, at a length of  $\sqrt{2}a$ . The ratio of the longest streamtube length over the shortest is  $\sqrt{2}$ . The average width of the longest streamtube is obtained by equating volumetric flowrates in the longest and shortest streamtubes, substituting Darcy's Law, employing the result above regarding the lengths of the longest and shortest streamtubes, and canceling identical terms such as pressure drop. Hence, the average width of the longest streamtube is also  $\sqrt{2}$  times as great as the shortest streamtube and it follows that the volume of the longest streamtube is twice that of the shortest.

However, for a staggered-line-drive pattern with  $d/a = 1$ , the ratio of the length along the boundary ( $3a/2$ ) over the diagonal ( $\sqrt{5}a/2$ ) is  $3/\sqrt{5} \approx 1.34$ . From the streamline distribution in Fig. 5, we know that the shortest streamline is longer than diagonal<sup>5</sup>, and therefore the ratio of the longest streamline over the shortest is less than 1.34. This ratio is about 1.3 and, therefore, less than that for a five-spot pattern which is 1.41. The streamlines are more evenly distributed in the staggered-line-drive than in a five-spot pattern. Therefore, when the shortest streamtube breaks through, a larger portion of the other streamtubes have been swept in a staggered-line-drive than in a five-spot pattern. When  $d/a$  increases, the streamtube length ratio (longest to shortest) decreases. When breakthrough happens in the shortest streamtube, a greater portion is swept in the longest streamtube resulting in higher sweep efficiency at breakthrough.

#### Five-Spot Pattern, Very Favorable Mobility Ratio

For a favorable mobility ratio ( $M < 1$ ), the displacement is stable. For equal volumetric flow rate streamtubes, Eq. 10 holds. Here, we consider the case of very favorable mobility ratio, i.e., the displacing fluid viscosity is much higher than that of the displaced fluid. When the front moves a portion of the way down the streamtube, the pressure drop is mainly in the displacing phase. After a short injection time (compared to breakthrough), the pressure drop in the displaced phase is negligible. Therefore, Eq. 10 can be simplified to the following form

$$\int_0^{l_i} \frac{1}{w} dl \cong C(t) \quad (12)$$

In this extreme case, the displacement front is not influenced by the producer until the front is very close to the producer because the pressure drop between the front and the well plays a negligible role in the displacement (c.f., ref <sup>10</sup> for a discussion of cusping when  $M$  is near but not equal to 0). Initially, flow around the injector is radial, because the pattern appears to be infinite at short times. For example, examine Fig. 6b for  $t_D = 0.583$ . However, after the front reaches a corner of the pattern, the no-flow boundary condition along pattern borders alters the radial flow pattern. Pressure isobars must intersect the no-flow boundaries at  $90^\circ$ . This constrains the streamlines in the region adjacent to a boundary to be parallel to the boundary. Because the fluids are incompressible, streamlines cannot terminate. The flow field in the region near the front transitions from radial to quasi-radial. From the figure, we also see that streamtubes ahead of the front are narrower along the boundary than those in the center, which makes the front in the boundary

streamtubes move faster than in the central streamtubes. Little area is unswept and the sweep efficiency at breakthrough approaches unity.

As in the previous discussion, a long streamtube must be wider in the swept region, as compared to a short streamtube, in order to maintain equal resistance (same flow rate and pressure drop) in all streamtubes. Therefore, the streamtubes along the boundary widen near the corners. Streamlines must remain smooth as is apparent in Fig. 6b.

In summary, the very favorable mobility ratio conspires with boundary conditions to determine streamline paths and displacement patterns. Since the mobility ratio is very favorable, the displacement front is not influenced by the production well and remains very similar in shape to the pressure isobars until immediately prior to breakthrough. Thus, sweep efficiency at breakthrough is near unity.

#### Staggered Line Drive, Very Favorable Mobility Ratio

For the staggered-line-drive pattern, the displacement at the beginning is similar to that in the five-spot pattern. That is, the displacement pattern is radial around the injector before the front reaches the nearest corner. The differences in displacement behavior between the two patterns occurs after the front reaches the near corner. For a five spot, because of the symmetry, the front reaches the two corners at the same time. However, for a staggered line drive, the front reaches the closest corner first.

After the front passes the near corner, the streamlines evolve in a way similar to the five spot. The streamtubes along the boundary are wide near the corner but narrow near the front. This makes the front near the boundary move faster because the streamtubes are narrower than those in the center of the pattern. Therefore, the front near the boundary on the near no-flow corner side catches up, and the displacement approaches linear flow (see the relevant streamline distribution in Fig. 7 at  $t_D = 0.60$  and  $0.80$ ). If the aspect ratio is large, flow in the center of the pattern must become nearly linear because the pressure isobars are nearly straight and intersect the pattern boundary at  $90^\circ$ .

Similar to the discussion above for a five-spot pattern, for a very favorable mobility ratio, the displacing front is perpendicular to the borders of the pattern both before and after the front passes the nearest corner. As a result, we see linear displacement for some time until the front on the near-corner side approaches the producer as shown in Fig. 7.

When the front approaches the producer, the streamtubes narrow due to the confinement of the pattern boundary and the well. And therefore, with the same flow rate, the displacing fluid will break through relatively quickly in the streamtubes closest to the producer. The front on the far no-flow side progresses more slowly. This streamline distribution does not change greatly as the mobility ratio becomes more favorable. Sweep out of the pattern is not complete at breakthrough. For instance, a small amount of the resident fluid remains along the right hand boundary as shown by the saturation distribution in Fig 7a at  $t_D = 0.94$ .

If the length of staggered line drive is increased (increasing  $d/a$ ), then the displacement will approach linear flow and the sweep efficiency at breakthrough will approach unity. The proportion of unswept area decreases as  $d/a$  increases.

With the piston-like displacement behavior now well understood, an obvious extension of this work is to consider sweep efficiency for the more general case of non piston-like displacements. For displacements with  $M$  close to 1, we expect that fractional flow versus time curves at the producer could become more spread as the amount of oil displaced by the front decreases and significant oil production from each streamtube continues after breakthrough.

However, for very favorable mobility ratios, the large viscosity of the displacing phase dominates displacement behavior. It is very hard to achieve a displacement front that is not piston like in this limit. Recovery from a five-spot pattern will remain near 1 at breakthrough for very favorable mobility ratios.

## CONCLUSIONS

Pattern performance changes with mobility ratio. For unit mobility ratio, unfavorable mobility ratios and some favorable mobility ratios ( $M > 0.3$ ), a common staggered-line-drive ( $d/a = 1$ ) pattern has larger areal sweep efficiency than a five-spot ( $d/a = 0.5$ ) pattern. However, for very favorable mobility ratios ( $M < 0.3$ ), a five-spot pattern has better sweep efficiency than a common staggered-line-drive.

The reason for this behavior is the evolution of the pressure distribution and the resulting streamlines with mobility ratio. For very favorable mobility ratios, the displacing front nearly parallels an isobar and intersects the pattern boundary at  $90^\circ$ . This causes the fronts at times near breakthrough to become radial around the producer for a five-spot pattern. This displacing front shape is due to the symmetry of the five-spot pattern.

For a staggered line drive undergoing displacement at a very favorable mobility ratio, the displacing front is also perpendicular to the border of the pattern. However, because the pattern is not symmetric, sweepout at breakthrough is not complete. Only in the limit of very large  $d/a$  will the areal sweep efficiency approach 1.

The simulation results are quite close to the analytical solutions for unit mobility ratio. The results are also very close to the experimental data, Dyes *et al*<sup>1</sup>, after breakthrough at various mobility ratios. We find physical dispersion in the Dyes *et al* experimental results that causes earlier breakthrough time.

We observed some numerical dispersion in our simulation results. For very favorable mobility ratios, the dispersion is small. We corrected the simulation results by fitting the fractional flow curves with second order polynomials to estimate breakthrough times.

## ACKNOWLEDGMENT

We thank R. P. Batycky, M. R. Thiele, and M. J. Blunt for making 3DSL available and for helpful discussions. This work was supported by the Assistant Secretary for Fossil Energy, Office of Oil, Gas, and Shale Technologies of the U.S. Department of Energy under contract No. DE-FG22-96BC14994 to Stanford University. Likewise, the support of the SUPRI-A Industrial Affiliates is gratefully acknowledged.

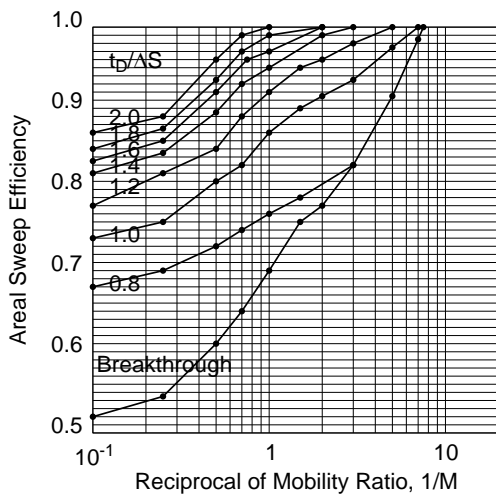
## NOMENCLATURE

$A$	area, $L^2$
$A_S$	area swept, $L^2$
$A_T$	total area of the pattern, $L^2$
$a$	distance between like wells (injection or production) in a row, $L$
$d$	distance between adjacent rows of injection and production wells, $L$
$E_A$	areal sweep efficiency
$f_w$	fractional flow of water
$h$	bed thickness, $L$

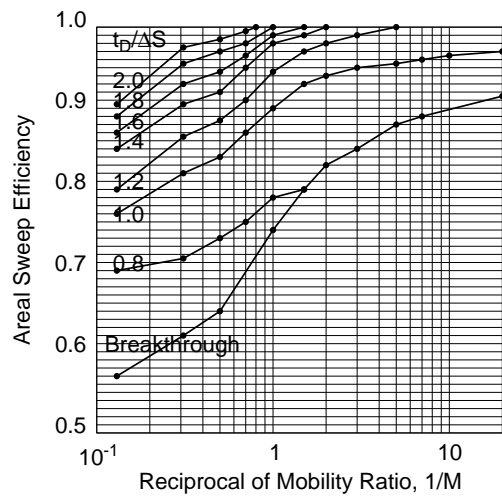
$k$	permeability, L <sup>2</sup>
$k_{ro}$	relative permeability of oil
$k_{rw}$	relative permeability of water
$l$	length, L
$L_i$	length of stream tube i, L
$l_{fi}$	distance of the displacing front from the injector in stream tube i, L
$M$	mobility ratio
$p$	pressure, M/L • T <sup>2</sup>
$q$	flow rate, L <sup>3</sup> /T
$R_i$	flow resistance of stream tube i, M/L <sup>4</sup> • T
$S$	saturation
$S_w$	water saturation
$t_D$	dimensionless time
$V_I$	volume of displacing phase injected, L <sup>3</sup>
$w$	width of a stream tube, L
$\phi$	porosity
$\mu$	viscosity, M/L • T

#### REFERENCES

1. Dyes, A.B., B.H. Caudle, and R.A. Erickson, "Oil Production after Breakthrough--as Influenced by Mobility Ratio," Petroleum Transactions AIME, 201, 27-32, (1954).
2. Craig, F.F.Jr., The Reservoir Engineering Aspects of Water Flooding, Society of Petroleum Engineers Monograph, Dallas, TX, 1971.
3. Lake, L.W., Enhanced Oil Recovery, Prentice Hall Inc., Englewood Cliffs, NJ, 1989.
4. Morel-Seytoux, H.J., "Unit Mobility Ratio Displacement Calculations for Pattern Floods in Homogeneous Medium," Soc. Pet. Eng. J., 6, 217-227, (1966).
5. Prats, M., "The Breakthrough Sweep Efficiency of the Staggered Line Drive," Trans. AIME, 207, 67-68, (1956).
6. Batycky, R.P., M.J. Blunt, and M.R. Thiele: "A 3D Streamline Simulator with Gravity and Changing Well Conditions," SPE 36726, in Proceedings of the Soc. Pet. Eng. Ann. Tech. Conf. and Exhibition, Denver, CO (Oct. 1996).
7. Thiele, M.R., R.P. Batycky, M.J. Blunt, and F.M. Orr Jr., "Simulating Flow in Heterogeneous Systems Using Streamtubes and Streamlines," Soc. Pet. Eng. Res. Eng., 11, 5-12, (1996).
8. Wang, Y., "A Study of the Effect of Mobility Ratios on Pattern Displacement Behavior and Streamlines to Infer Permeability Fields", MS Report Dept of Petroleum Engineering, Stanford University, 1998.
9. Peaceman, D.W., Fundamentals of Numerical Reservoir Simulation, Elsevier Scientific Publishing Co., New York, 1977.
10. Claridge, E.L., "Prediction of Recovery in Unstable Miscible Flooding," Soc. Pet. Eng. J., 12, 143-155, (1972).

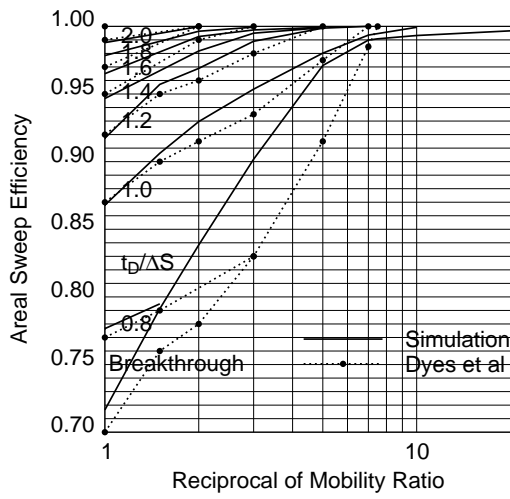


(a) Five Spot Pattern

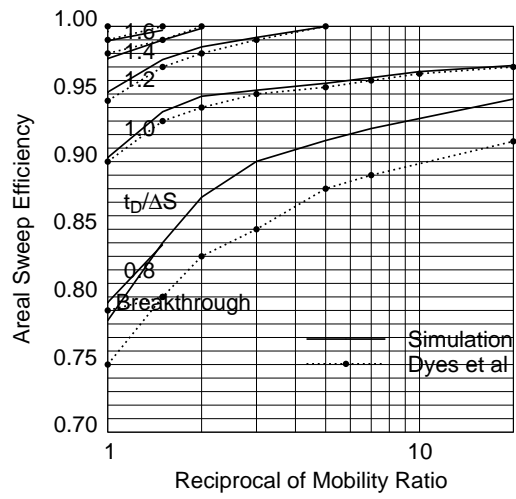


(b) Staggered Line Drive,  $d/a = 1$

FIG. 1 Dyes et al experimental areal sweep results.



(a) Five Spot Pattern



(b) Staggered Line Drive,  $d/a = 1$

FIG. 2 Comparison of simulated and experimental areal sweep behavior

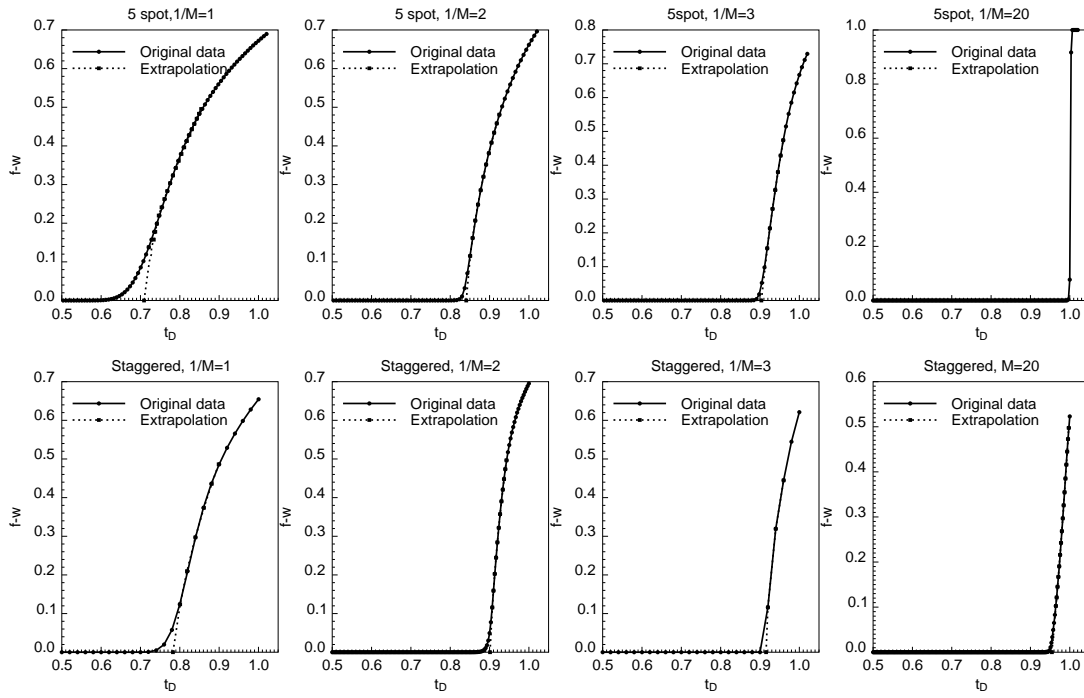


FIG 3. Fractional flow versus dimensionless time at producer  
 -- determination of breakthrough time

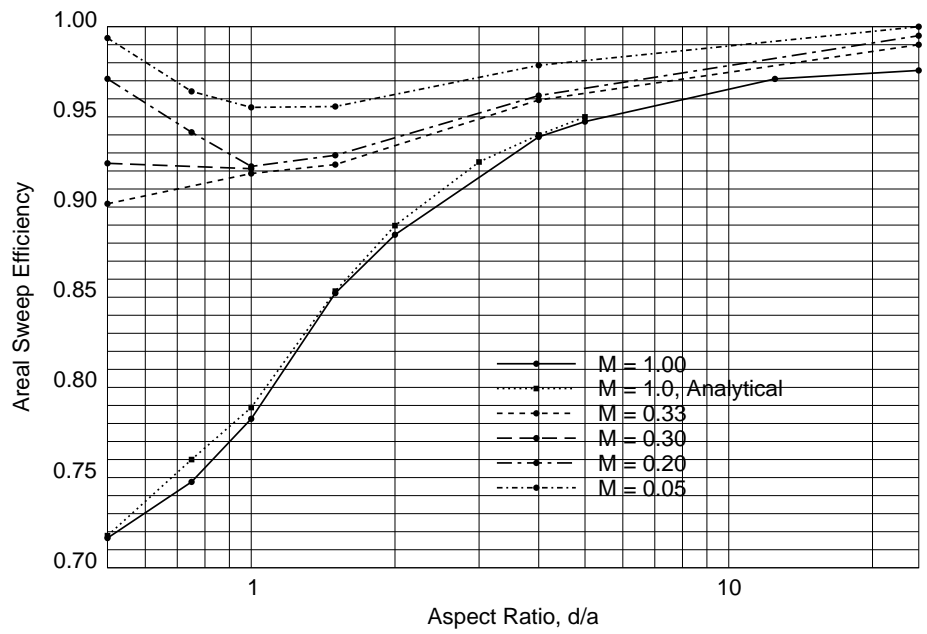
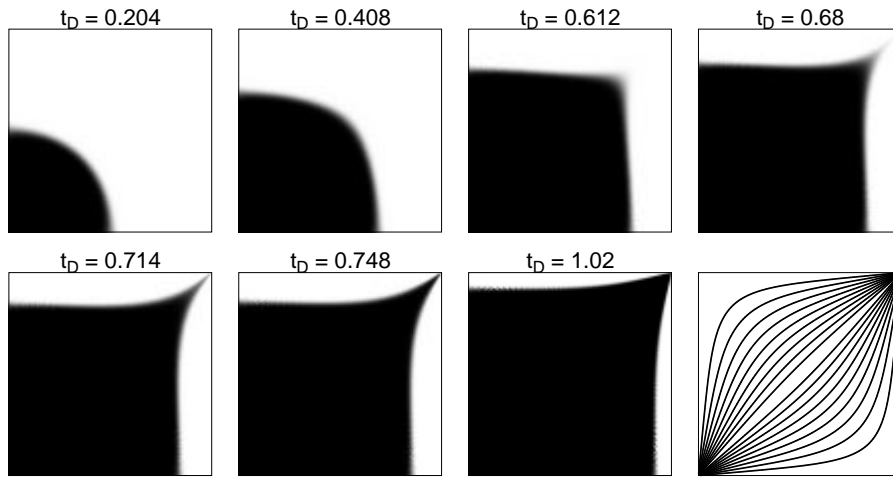
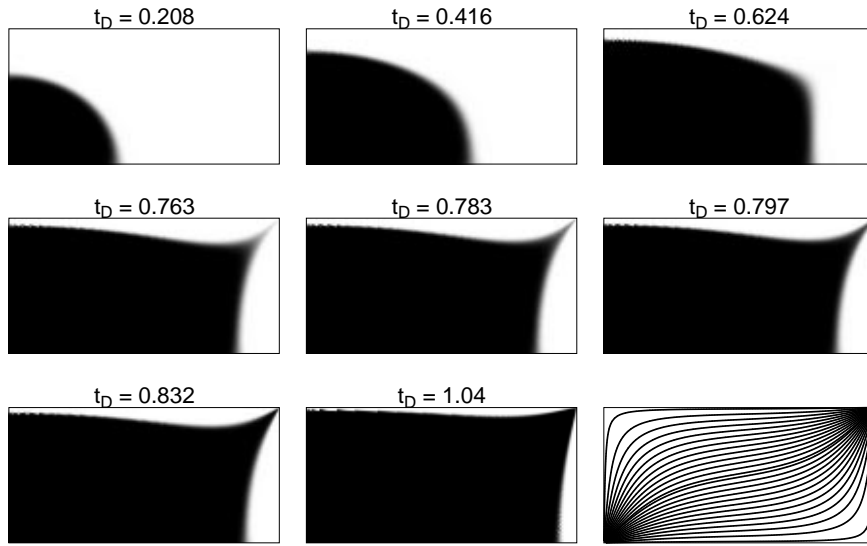


FIG. 4 Effect of mobility ratios and pattern geometry on areal sweep efficiency at breakthrough.

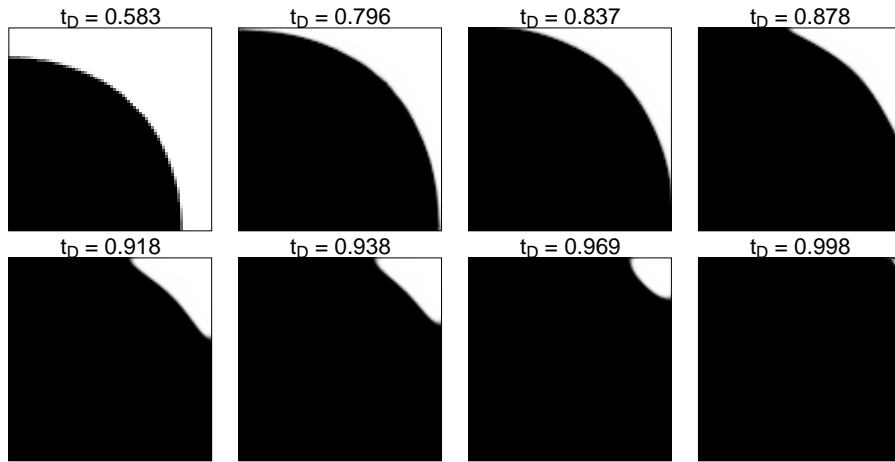


(a) Five Spot Pattern

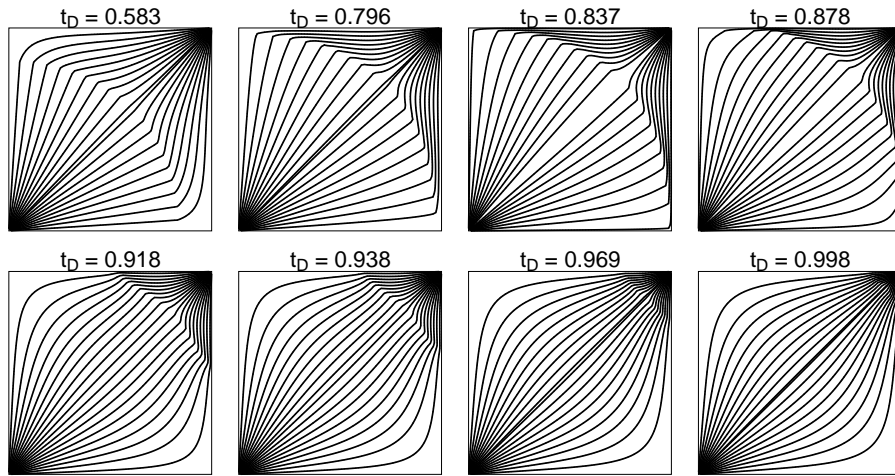


(b) Staggered Line Drive

FIG. 5 Streamline and saturation distributions, unit mobility ratio.



(a) Saturation Distribution



(b) Streamline Distribution

FIG. 6 Five-spot pattern, very favorable mobility ratio,  $1/M = 20$ .

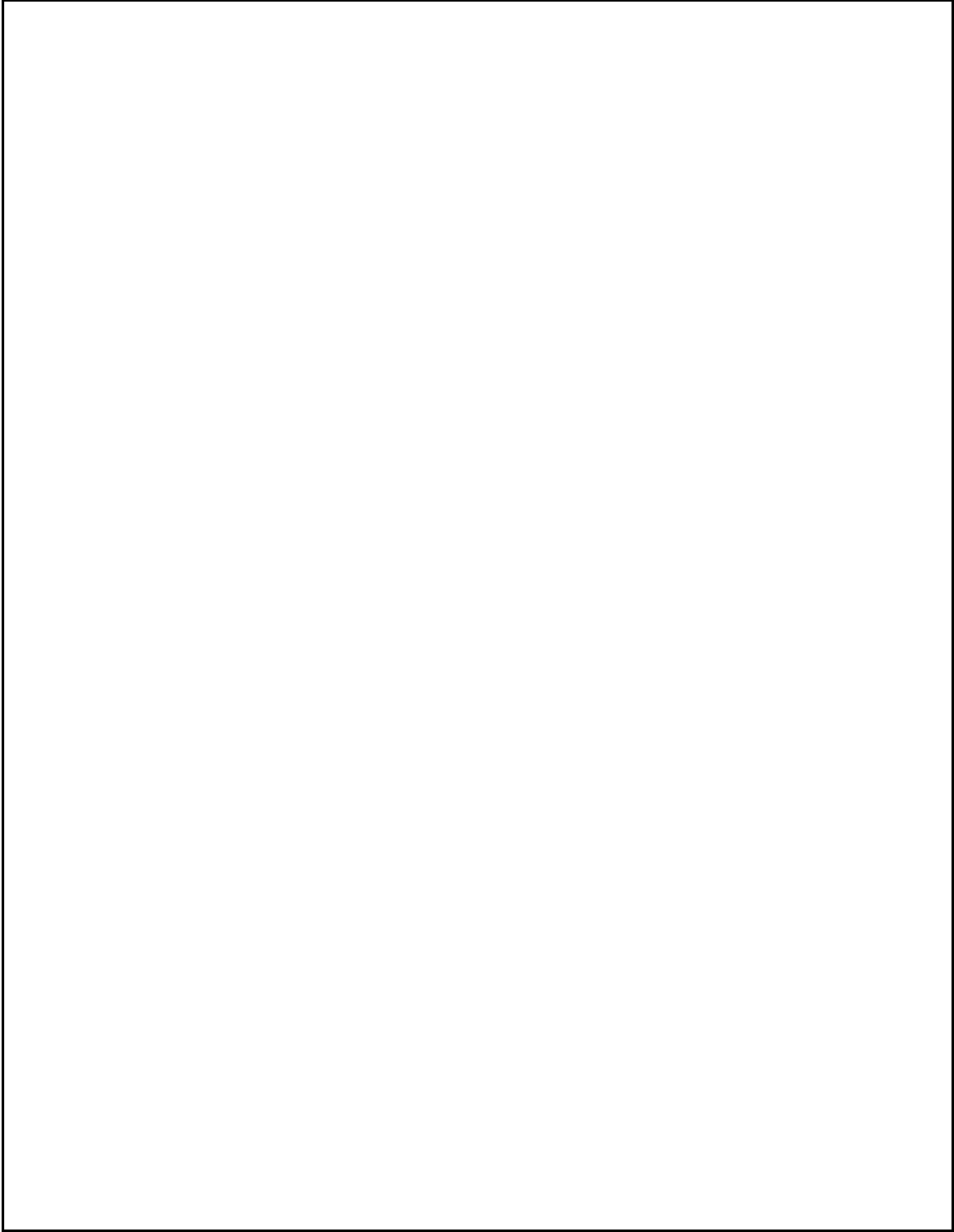


FIG. 7 Staggered-line-drive pattern, very favorable mobility ratio,  $1/M = 20$ .